

Quasi-linear theory of forced magnetic reconnection for the transition from linear to Rutherford regime

Wenlong HUANG

School of Computer Science and Technology,
Anhui Engineering Laboratory for Industrial Internet Intelligent Applications and
Security, Anhui University of Technology, Ma'anshan, Anhui 243002, China

Ping ZHU

International Joint Research Laboratory of Magnetic Confinement Fusion and
Plasma Physics, State Key Laboratory of Advanced Electromagnetic Engineering and
Technology, School of Electrical and Electronic Engineering, Huazhong University of
Science and Technology, Wuhan, Hubei 430074, China
Department of Engineering Physics, University of Wisconsin-Madison, Madison,
Wisconsin 53706, USA

E-mail: zhup@hust.edu.cn

Abstract. Using the in-viscid two-field reduced MHD model, a new analytical theory is developed to unify the Hahm-Kulsrud-Taylor (HKT) linear solution and the Rutherford quasi-linear regime. Adopting a quasi-linear approach, we obtain a closed system of equations for plasma response in a static plasma in slab geometry. An integral form of analytical solution is obtained for the forced magnetic reconnection, uniformly valid throughout the entire regimes from the HKT linear solution to the Rutherford quasi-linear solution. In particular, the quasi-linear effect can be described by a single coefficient $K_s \propto S^{8/5} \psi_c^2$, where $S = \frac{\tau_R}{\tau_A}$ and ψ_c are the Lunquist number and amplitude of external magnetic perturbation, respectively. The HKT linear solution for response can be recovered when the index $K_s \rightarrow 0$. On the other hand, the quasi-linear effect plays a key role in the island growth when $K_s \sim 1$. Our new analytical solution has also been compared with reduced MHD simulations with agreement.

1. Introduction

In the last decades, three dimensional external magnetic coils have been widely equipped in various fusion devices due to the emerging and promising potential for controlling plasma activities [1, 2, 3, 4]. For example, various MHD instabilities, such as edge localized modes (ELMs), can be suppressed or mitigated by resonant magnetic perturbation (RMP) coils [5, 6, 7, 8, 9, 10]. Recent experimental and theoretical results show that the mechanism of ELM suppression or mitigation by RMPs is connected with the forced magnetic reconnection (FMR) processes on resonant surfaces in the pedestal region [11, 12, 13, 14].

According to the island width, which is decided by the amplitude of RMP, there are several different models of FMR. When the island width (W) is much narrower than the resistive layer width (δ_{layer}), quasi-linear magnetic terms can be neglected. In this regime, Hahm and Kulsrud proposed the linear FMR solution in the Taylor problem (HKT) [15]. Later, the linear HKT solution in the resistive-inertial (RI) regime was extended to include the steady state plasma flow [16]. It should be noted that the plasma flow can also be dramatically modified by RMPs even in the regime where $W \ll \delta_{\text{layer}}$ [17, 18, 19]. To study the plasma response in the small island regime, a quasi-linear model for plasma flow response to RMPs in a tokamak has been self-consistently developed purely from the two-field reduced MHD model [20, 21].

When $W \sim \delta_{\text{layer}}$, the forced island enters into the Rutherford regime [15, 22]. In the Rutherford regime, the FMR model is constitute of the island evolution, torque balance equation, and phase condition [23]. This model has been used to study magnetic island control using RMPs [24, 25, 26]. Recently, an extended FMR model with neo-classical and two-fluid effects [12] is used to simulate the RMP-induced ELM suppression experiments in DIII-D [27]. Predictions from those theory models are highly relevant to the interpretation of experimental results on the RMP-induced ELM suppression [13, 14].

Physically, the linear theory should be recovered from the quasi-linear one when the related effect tends to zero. However, one can find that the linear HKT solution cannot be reduced from the FMR model in the Rutherford regime in all those theories mentioned above [12, 16, 24, 25, 28]. To make a better understanding of FMR, an unified theory uniformly connecting the HKT and Rutherford regimes may be needed. On the other hand, a quasi-linear theory was proposed to reproduce the Rutherford equation and unify the linear exponential and quasi-linear algebraic growth of intrinsic tearing mode [29]. Nonetheless, one of the necessary assumptions used in the derivation, e.g. the expression of the perturbed stream function, may be not appropriate for FMR [15]. To uniformly connecting the HKT linear and Rutherford quasi-linear solutions of FMR, we should extend the previous quasi-linear approach.

In this work, we propose a new analytical theory to unify the HKT linear solution and the Rutherford quasi-linear regime based on the in-viscid two-field reduced MHD model [30]. Adopting Li's quasi-linear approach [29], we obtain a closed system of

equations for plasma response in the Taylor problem. Transforming the term of quasi-linear perturbed current into the exponential parts of ψ_1 (the perturbed flux function) and ϕ_1 (the perturbed stream function) and using the Laplace transformation, we obtain an integral form of analytical solution for FMR, which uniformly connect the HKT linear and Rutherford quasi-linear solutions. From the solution of FMR, we find that the quasi-linear effect can be described by a single coefficient $K_s \propto S^{8/5} \psi_c^2$, where $S = \frac{\tau_R}{\tau_A}$ and ψ_c are the Lunquist number and amplitude of external magnetic perturbation, respectively. The HKT linear solution for response can be recovered when the index K_s tends to zero. On the other hand, the quasi-linear effect plays a key role on the island growth when $K_s \sim 1$. To analyze the FMR solution, we numerically solve the final expression the normalized flux function ψ_{norm} . Numerical results show that ψ_{norm} decreases with K_s since the quasi-linear effect is always negative. Our new analytical solution also has been verified by reduced MHD simulation.

Note that we derive the FMR solution in a static plasma in slab geometry. In such an equilibrium, we can make an exactly comparison between the analytical solution and numerical simulation. Our work can be straightforwardly extended to the cylindrical geometry. On the other hand, our work is appropriate in the regime where effects of the plasma flow and viscosity can be neglected. In the rotating plasma, FMR solution obtained in this work should be improved. Even though, our work may provide a necessary foundation to the building of the unified plasma response model including plasma flow and viscosity effects.

The rest of the paper is organized as follows. In Sec. 2, we introduce the reduced MHD model of the Taylor problem. Sec. 3 is devoted to the analytical derivation and numerical analysis of the FMR solution. Verification of the analytical solution of FMR by reduced MHD simulation is given in Sec. 4. Finally, we give a summary and discussion in Sec. 5.

2. Model of the reduced MHD equations

In this work, we study the FMR response induced by external magnetic perturbations in a low- β plasma based on the two-field reduced MHD model. Using a Cartesian coordinate system (x, y, z) and introducing the flux function ψ and stream function ϕ , the magnetic field and the velocity can be written as $\vec{B} = B_T \vec{e}_z + \vec{e}_z \times \nabla \psi$ and $\vec{v} = \vec{e}_z \times \nabla \phi$, where B_T is the toroidal magnetic field. The incompressible two-field reduced MHD model governing ψ and F are given, respectively, by

$$\frac{\partial \psi}{\partial t} + (\vec{e}_z \times \nabla \phi) \cdot \nabla \psi - B_T \partial_z \phi = \eta J_z, \quad (1)$$

$$\rho \left(\frac{\partial}{\partial t} + \vec{v} \cdot \nabla \right) F = \vec{B} \cdot \nabla J_z, \quad (2)$$

$$(3)$$

where

$$F = \vec{e}_z \cdot \nabla \times \vec{v} = \nabla_{\perp}^2 \phi = \left[\frac{\partial^2}{\partial x^2} + \frac{\partial^2}{\partial y^2} \right] \phi, \quad (4)$$

$$J_z = \vec{e}_z \cdot \vec{J} = \frac{1}{\mu_0} \nabla_{\perp}^2 \psi = \frac{1}{\mu_0} \left[\frac{\partial^2}{\partial x^2} + \frac{\partial^2}{\partial y^2} \right] \psi, \quad (5)$$

and ρ and η are the plasma density and resistivity, respectively. In the Taylor problem, the plasma is surrounded by perfect conducting walls at $x = \pm a$ and the boundary perturbation is specified as $x = \pm(a - \delta_{\text{RMP}} e^{iky})$, where δ_{RMP} is the static boundary displacement [15]. The plasma equilibrium are set as $B_T = 0$, $v_{\text{eq}} = 0$, and $B_{\text{peq}} = B_p \frac{x}{a}$ in the 2-D Taylor problem. Then, the equilibrium toroidal current $J_{\text{zeq}} = \frac{1}{\mu_0} \frac{B_p}{a}$ is a constant.

3. Integral solution of the FMR and its numerical analysis

In this work, we define $\psi = \psi_{\text{eq}} + \delta\psi$, $\phi = \delta\phi$, $\delta\psi = \sum_{l=0}^{\infty} \delta\psi_l = \delta\psi_0 + \sum_{l=1}^{\infty} \psi_l \cos(lky)$, and $\delta\phi = \sum_{l=0}^{\infty} \delta\phi_l = \delta\phi_0 + \sum_{l=1}^{\infty} \phi_l \sin(lky)$. Then, Eqs. (1) and (2) can be reduced to the following forms if one neglects the effects of higher harmonic coupling and plasma flow induced by RMPs

$$\partial_t \delta\psi_1 + \underbrace{\delta \vec{v}_1 \cdot \nabla \psi_{\text{eq}} + \delta \vec{v}_1 \cdot \nabla \delta\psi_0}_{\text{QLMA}} = \eta \delta J_{z1}, \quad (6)$$

$$\underbrace{\rho \partial_t \delta F_1}_{\text{ITV}} = \vec{B}_{\text{eq}} \cdot \nabla \delta J_{z1} + \underbrace{\delta \vec{B}_1 \cdot \nabla J_{\text{zeq}}}_{\text{EQJD}} + \underbrace{\delta \vec{B}_0 \cdot \nabla \delta J_{z1}}_{\text{QLMB}} + \underbrace{\delta \vec{B}_1 \cdot \nabla \delta J_{z0}}_{\text{QLJ}}, \quad (7)$$

$$\underbrace{\partial_t \delta\psi_0}_{\text{QLMC}} + \langle \delta \vec{v}_1 \cdot \nabla \delta\psi_1 \rangle = \eta \delta J_{z0}, \quad (8)$$

where $\langle f \rangle = \frac{1}{2\pi} \int_0^{2\pi/k} f dy$. For the convenience of discussion, we mark the quasi-linear magnetic and current terms as QLMA, QLMB, and QLMC and QLJ in Eqs. (6)-(8). To solve the above quasi-linear Eqs. (6)-(8), QLMC should be neglected at first [29]. If one neglects the terms of ITV, QLMA, and QLMB in Eqs. (6) and (7) and adopt the certain assumption of ϕ_1 (see also in Appendix B), the Rutherford equation can be recovered [22]. When ITV in Eq. (7) is included, one can unify the linear exponential and quasi-linear algebraic growth of intrinsic tearing mode. In addition, the terms of QLMA and QLMB should be contained only if $W \Delta' \gg 1$ [29], where $\Delta' = [\frac{1}{\psi_s} \frac{d\psi_1}{dx}]_{x=0}$ is the tearing index and $[f]_{x=0}$ is the jump across the tearing layer around the resonant surface [35].

3.1. Integral form of the analytical FMR solution

In the outer region, we neglect the non-ideal and quasi-linear terms. Then, solution of Eq. (7) is

$$\psi_1 = [\cosh(kx) - \frac{\sinh(kx)}{\tanh(ka)}] \psi_s + [\frac{\sinh(kx)}{\sinh(ka)}] \psi_c, \quad (9)$$

where $\psi_s = \psi_1(0)$ and $\psi_c = \psi_1(x = \pm a) = B_p \delta_{\text{RMP}}$. From Eq. (9), we can rewrite Δ' as $\psi_s \Delta' = \psi_s \Delta'_0 + B_p \delta_{\text{RMP}} \Delta'_e = \frac{-2k}{\tanh(ka)} \psi_s + \frac{2k}{\sinh(ka)} \psi_c$.

In the inner region, $\partial_x \gg k$ is assumed. Within appropriate amplitude of the boundary perturbation [15, 31, 32], the constant- ψ assumption is valid. Note that EQJD = 0 in our equilibrium. Then, Eqs. (6)-(8) in the inner region can be simplified to

$$\partial_t \psi_1 - k B_p \frac{x}{a} \phi_1 = \eta J_{z1}, \quad (10)$$

$$\rho \partial_t F_1 = -k B_p \frac{x}{a} J_{z1} - \frac{k^2}{2\eta} \psi_1^2 \partial_x^2 \phi_1. \quad (11)$$

Here, QLMA and QLMB are neglected since $B_{\text{peq}} = \partial_x \psi_{\text{eq}} \gg \delta B_{p0} = \partial_x \delta \psi_0$. This approximation will be verified by reduced MHD simulation in the Sec. 4.2.

Since the term of EQJD in Eq. (7) is essential only when the mode is close to marginality [33, 34]. For similar reasons, neither has been considered in the classical theory of resistive tearing mode [22, 35]. Then, Eqs. (10) and (11) can be straightforwardly extended to the cylindrical geometry.

In 1995, Li proposed a quasi-linear approach to reproduce the Rutherford equation and unify the linear exponential and quasi-linear algebraic growth of intrinsic tearing mode by assuming $\phi_1 \propto \partial_t \psi_s \Phi(x)$ (see also in Appendix B) [29]. Nonetheless, such an assumption may be not appropriate for FMR even in the linear limit (see also in Appendix C). Different with [29], we do not take assumptions on the expression of ϕ_1 . Instead, Eqs. (10) and (11) in the inner region are solved using the Laplace transform.

Following [20], we define $f_1 = \hat{f}_1 e^{-\varphi_{\text{temp}}}$, where $S = \frac{\tau_R}{\tau_A}$, $K = \frac{k^2}{B_p^2} S^{\frac{8}{5}}$, and $\varphi_{\text{temp}} = \int_0^t \frac{k^2}{2\rho\eta} \psi_s^2(t') dt' = \frac{1}{2} K \int_0^\tau \psi_s^2(\tau') d\tau'$. Then, we transform Eqs. (10) and (11) to the following forms

$$\partial_t \hat{\psi}_1 - \frac{k^2}{2\rho\eta} \psi_s^2 \hat{\psi}_1 - k B_p \frac{x}{a} \hat{\phi}_1 = \eta \hat{J}_{z1}, \quad (12)$$

$$\rho \partial_t \hat{F}_1 = -k B_p \frac{x}{a} \hat{J}_{z1}. \quad (13)$$

Introducing the Laplace transform [15], we convert Eqs. (12) and (13) to

$$\frac{\partial^2}{\partial \chi^2} \Psi = \delta_{\text{RI}} \Omega (G + \chi U), \quad (14)$$

$$\frac{\partial^2}{\partial \chi^2} U - \chi^2 U = \chi G, \quad (15)$$

where

$$\begin{aligned} \tau_R &= \frac{\mu_0 a^2}{\eta}, \tau_A = \frac{a}{B_p / \sqrt{\mu_0 \rho}}, \delta_{\text{RI}}^4 = \frac{s \tau_A^2}{(ka)^2 \tau_R}, \nu = \frac{s}{k^2 \delta_{\text{RI}}}, \Omega = \delta_{\text{RI}} \tau_R s, \chi = \frac{x}{\delta_{\text{RI}} a}, \\ \Psi_s &= \frac{k}{B_p} \tilde{\psi}_s, \Psi_c = \frac{k}{B_p} \tilde{\psi}_c, G = \frac{k}{B_p} \tilde{g}, U = -\tilde{\phi} / \nu, \\ s \tilde{g} &= s \tilde{\psi}_s - \mathcal{L} \left[\left(\frac{k^2}{2\rho\eta} \psi_s^2 \right) \hat{\psi}_s \right], \end{aligned}$$

$$\begin{aligned}\tilde{\psi} &= \mathcal{L}[\hat{\psi}_1] = \int_0^\infty \hat{\psi}_1 e^{-st} dt, \\ \tilde{\phi} &= \mathcal{L}[\hat{\phi}_1] = \int_0^\infty \hat{\phi}_1 e^{-st} dt.\end{aligned}$$

In [29], Li unify the linear exponential and quasi-linear algebraic growth of tearing mode. Following their quasi-linear approach, we propose an integral form of FMR response which unify HKT linear and Rutherford quasi-linear solutions. Furthermore, Eq. (15) can be converted to Eq. (B.8) if we define $U = YG$. Nonetheless, the final expressions of ϕ_1 are different from our work (Eq. (C.4)) and previous one (Eq. (C.1)).

Via the asymptotic matching, we arrive at

$$\frac{3\Omega}{\sqrt{2}r_s}G = \Delta'_0\Psi_s + \Delta'_e\Psi_c. \quad (16)$$

To obtain a transparent solution, we rearrange Eq. (16) to

$$\Psi_s = \frac{\Delta'_e}{-\Delta'_0} \frac{\Psi_c}{1 + \lambda p^{\frac{5}{4}}} + \frac{1}{2} \frac{K}{p} \left\{ 1 - \frac{1}{1 + \lambda p^{\frac{5}{4}}} \right\} \mathcal{L}[\psi_s^2 \hat{\psi}_s], \quad (17)$$

where $p = s\tau_R^{\frac{3}{5}}\tau_A^{\frac{2}{5}}$ and $\lambda = \frac{3}{-2ka\Delta'_0} [\frac{1}{4(ka)^2}]^{\frac{1}{4}}$. Then, the following expression of ψ_s can be obtained by the inverse Laplace transform

$$\begin{aligned}\psi_s(\tau) &= \frac{\Delta'_e}{-\Delta'_0} e^{-\varphi_{\text{temp}}(\tau)} \int_0^\tau G(\tau - \tau') \psi_c(\tau') e^{\varphi_{\text{temp}}(\tau')} d\tau' + \frac{1}{2} K e^{-\varphi_{\text{temp}}(\tau)} \int_0^\tau \psi_s^3(\tau') e^{\varphi_{\text{temp}}(\tau')} d\tau' \\ &\quad - \frac{1}{2} K e^{-\varphi_{\text{temp}}(\tau)} \int_0^\tau H(\tau - \tau') \psi_s^3(\tau') e^{\varphi_{\text{temp}}(\tau')} d\tau',\end{aligned} \quad (18)$$

where

$$\begin{aligned}G(\tau) &= -\frac{4}{5} [P_A e^{P_A \tau} + P_B e^{P_B \tau}] - \frac{\lambda}{\sqrt{2}\pi} \int_0^\infty e^{-u\tau} \frac{u^{\frac{5}{4}}}{(1 - \sqrt{2}\lambda u^{\frac{5}{4}} + \lambda^2 u^{\frac{5}{2}})} du, \\ H(\tau) &= 1 - \frac{4}{5} [e^{P_A \tau} + e^{P_B \tau}] + \frac{\lambda}{\sqrt{2}\pi} \int_0^\infty e^{-u\tau} \frac{u^{\frac{1}{4}}}{(1 - \sqrt{2}\lambda u^{\frac{5}{4}} + \lambda^2 u^{\frac{5}{2}})} du,\end{aligned}$$

and $P_A = \lambda^{-\frac{4}{5}} \exp(+\frac{4\pi i}{5})$, $P_B = \lambda^{-\frac{4}{5}} \exp(-\frac{4\pi i}{5})$, $\tau = t/(\tau_R^{3/5} \tau_A^{2/5})$.

The above integral form of analytical FMR solution, i.e. Eq. (18), is uniformly valid throughout the entire regimes from the HKT linear to the Rutherford quasi-linear regimes. Note that the linear solution can not be reduced from the modified Rutherford theory with RMP effect [15] since the term of ITV in Eq. (7) is neglected in the previous study [22]. On the other hand, one cannot expect that the unified theory uniformly connecting HKT linear and Rutherford quasi-linear solution can be obtained directly setting $\psi_s \Delta' = \psi_s \Delta'_0 + \psi_c \Delta'_e$ in Eq. (B.23) since $\phi_1 \propto \partial_t \psi_s \Phi(x)$, which is one of the necessary assumption in [29], may be not appropriate for FMR even in the linear limit.

To take a further step, we define $\psi_{\text{norm}} = \frac{-\Delta'_0}{\Delta'_e} \frac{\psi_s}{\psi_c}$, $K_s = \frac{1}{2} (\frac{\Delta'_e}{-\Delta'_0})^2 K \psi_c^2$, $\varphi_s(\tau) = \int_0^\tau \psi_{\text{norm}}^2(\tau') d\tau'$, and $\varphi_{\text{temp}} = K_s \varphi_s(\tau)$. Then, Eq. (18) can be rearranged to

$$\psi_{\text{norm}}(\tau) = \int_0^\tau G(\tau - \tau') e^{\varphi_K(\tau, \tau')} d\tau' + K_s \int_0^\tau [1 - H(\tau - \tau')] \psi_{\text{norm}}^3(\tau') e^{\varphi_K(\tau, \tau')} d\tau'$$

$$\begin{aligned}
 &= \underbrace{\int_0^\tau G(\tau - \tau') d\tau'}_{\text{LIN}} + \underbrace{\int_0^\tau G(\tau - \tau') \left\{ e^{\varphi_K(\tau, \tau')} - 1 \right\} d\tau'}_{\text{QLA}} + \\
 &\quad \underbrace{K_s \int_0^\tau [1 - H(\tau - \tau')] \psi_{\text{norm}}^3(\tau') e^{\varphi_K(\tau, \tau')} d\tau'}_{\text{QLB}}, \tag{19}
 \end{aligned}$$

where $\varphi_K(\tau, \tau') = K_s[\varphi_s(\tau') - \varphi_s(\tau)]$. To analyze the dynamics of FMR, we divide the expression of ψ_{norm} into three parts, i.e. LIN, QLA, and QLB. Here, LIN is the normalized HKT solution. QLA and QLB represent the quasi-linear effect. Further analysis will be shown in Sec. 3.2.

Note that $K_s = \frac{1}{2} \frac{k^2}{B_p^2} \left(\frac{\Delta'_e}{-\Delta'_0} \right)^2 \left(\frac{\tau_R}{\tau_A} \right)^{\frac{8}{5}} \psi_c^2$ can be viewed as the quasi-linear index. When $K_s \rightarrow 0$, the linear HKT solution is recovered [15]. Then, the normalized HKT linear solution is equivalent to Eq. (19) with $K_s = 0$. On the other hand, quasi-linear effect may play an important role if $K_s \sim 1$. Since $K_s \propto S^{8/5} \psi_c^2$, the quasi-linear effect increases with ψ_c and decreases with η .

Before we analyze the dynamics of FMR solution, it is useful to discuss the steady state solution of Eqs. (10) and (11). In fact, the steady state of ϕ_1 satisfies

$$\frac{\partial^2}{\partial x^2} \phi_1 - \frac{2B_p^2 x^2}{\psi_s^2 a^2} \phi_1 = 0. \tag{20}$$

A trivial solution of Eq. (20) is $\phi_1(x, t \rightarrow \infty) = 0$. Then, $J_{z1}(x, t \rightarrow \infty) = 0$. Via the asymptotic matching, the steady state expression of ψ_s satisfies $\psi_s = -\frac{\Delta'_e}{\Delta'_0} \psi_c$, or, $\psi_{\text{norm}} = 1$. Such a steady state solution can also be obtained from the modified Rutherford equation [15] and verified by numerical evaluation and reduced MHD simulation in the Secs. 3.2 and 4.2, respectively.

3.2. Numerical analysis of the FMR solution

In this subsection, we numerically evaluate Eq. (19) and analyze characteristics of FMR. Since the right hand side of Eq. (19) is an integral form of ψ_{norm} , we use the Gauss-Seidel iteration to obtain the numerical evaluation of ψ_{norm} . The basic parameters used here are $a = 0.5m$, $k = 1/a$, $\rho = 1.67 \times 10^{-8} kg/m^3$, and $B_p = 0.2T$.

In Fig. 1, we illustrate the dependence of K_s on the Lunquist number (RMP amplitude) for different δ_{RMP} (S) to display parameter regimes where $K_s \ll 1$ and $K_s \sim 1$. For example, $K_s \sim 1$ ($K_s \ll 1$) when $S \sim 2 \times 10^4$ ($S \ll 2 \times 10^4$) with $\delta_{\text{RMP}} = 4 \times 10^{-4}m$.

Time evolution of ψ_{norm} for different K_s is shown in Fig. 2. When $K_s = 0.5$, dynamics of the forced magnetic island is similar with the linear HKT solution. At first, ψ_{norm} rapidly grows with time. When τ is larger than a critical value, the forced island decreases and tends to a steady state. On the other hand, the overshoot behavior of ψ_{norm} gradually disappears with the increase of K_s . Instead, ψ_{norm} increases with τ and gradually evolves to the steady state. Due to the quasi-linear effect, the forced island width decreases with K_s . Besides, the steady state solutions in both the linear and

quasi-linear regimes satisfy $\psi_{\text{norm}} = 1$, which is consistent with our theoretical analysis in the last of Sec. 3.1.

To analyze the quasi-linear effect in further, we plot different parts of Eq. (19) in Fig. 3. In Fig. 3, QLA and QLB are negative and positive, respectively. Besides, $|\text{QLA}| \geq |\text{QLB}|$. Then, the net contribution of quasi-linear terms in Eq. (19) is always negative. Comparisons between the upper and lower panels of Fig. 3 show that $|\text{QLA} + \text{QLB}|$ increases with K_s . These findings explain why ψ_{norm} decreases with K_s in Fig. 2. On the other hand, $|\text{QLA}|$ and $|\text{QLB}|$ increase from 0 to their maximum values in the time scale $\tau \sim 3$. When $\tau \sim 10$, QLA and QLB are constants and canceled by each other. Then, as is shown in Fig. 2, the steady state of the normalized flux function is $\psi_{\text{norm}} = 1$.

4. Verification of the analytical model using reduced MHD simulation

In the Sec. 3, we propose an unified theory to connect the HKT linear and Rutherford quasi-linear FRM solutions. To verify the integral form of FMR solution in Eq. (19), we develop a two-field reduced MHD code.

4.1. Details of the two-field reduced MHD simulation code

In this subsection, we numerically solve the following quasi-linear reduced MHD model

$$\partial_t \delta\psi_1 + \delta\vec{v}_1 \cdot \nabla \psi_{\text{eq}} + \delta\vec{v}_1 \cdot \nabla \delta\psi_0 = \eta \delta J_{z1}, \quad (21)$$

$$\rho \partial_t \delta F_1 = \vec{B}_{\text{eq}} \cdot \nabla \delta J_{z1} + \delta \vec{B}_0 \cdot \nabla \delta J_{z1} + \delta \vec{B}_1 \cdot \nabla \delta J_{z0}, \quad (22)$$

$$\eta \delta J_{z0} = \langle \delta\vec{v}_1 \cdot \nabla \delta\psi_1 \rangle. \quad (23)$$

Here, QLMC is not included in Eq. (23). The boundary conditions for the stream function and flux function are $\phi_1(\pm a) = 0$ and $\psi_1(\pm a) = \psi_c$. Spatial derivatives are calculated by the second order central difference method. The time advance uses the prediction-correction method. The basic numerical parameters used here are $\Delta t = 1.82 \times 10^{-8} s$ and $\Delta x = 0.0025m$.

4.2. Simulation results

To compare with the analytical form of ψ_{norm} , the quasi-linear magnetic terms, i.e. QLMA, QLMB, and QLMC, are neglected at first.

The radial distributions of ϕ_1 and J_{z1} at different time are shown in Fig. 4. In Fig. 4, ϕ_1 and J_{z1} are odd and even functions of x , respectively. When $\tau \sim 2.83$, ϕ_1 and J_{z1} reach their maximum values. The perturbed quantities are vanished when $\tau \sim 8.55$. These two properties are consistent with Fig. 3. In particular, $J_{z1} \rightarrow 0$ when $\tau \sim 8.55$ indicates that the steady state solution of FMR is $\psi_{\text{norm}} = 1$, as is discussed in Sec. 3.

Comparison between theory and simulation results of ψ_{norm} for different K_s is shown in Fig. 5. The theoretical results are calculated from Eq. (19). As is shown in Eq. (19),

the quasi-linear effect could be described by a single coefficient K_s . To verify the integral form of ψ_{norm} , we scan η with fixed K_s in simulation. In the top ($K_s = 0$), middle ($K_s = 0.5$), and bottom ($K_s = 2$) panels of Fig. 5, simulation results for different η are all consistent with theoretical expression of ψ_{norm} . This fact indicates that the quasi-linear effect in the reduced MHD simulation can also be described by the quasi-linear coefficient K_s .

Next, terms of QLMA and QLMB are added in the simulation code. In the upper panel of Fig. (6), we find the simulation results with QLMA and QLMB for different η are also agree well with Eq. (19). This can be explained from Eqs. (21) and (22). In fact, the related terms in Eqs. (21) and (22) can be expressed as $\delta \vec{v}_1 \cdot \nabla \psi_{\text{eq}} + \delta \vec{v}_1 \cdot \nabla \delta \psi_0 = v_{1x}(B_{\text{peq}} + \delta B_{p0})$ and $\vec{B}_{\text{eq}} \cdot \nabla \delta J_{z1} + \delta \vec{B}_0 \cdot \nabla \delta J_{z1} = -k J_{z1}(B_{\text{peq}} + \delta B_{p0})$, where $\delta B_{p0} = \partial_x \delta \psi_0$. On the other hand, $B_{\text{peq}} \gg \delta B_{p0}$ in the quasi-linear stage. Then, QLMA and QLMB are not important for the island evolution. This conclusion is also verified in the lower panel of Fig. 6. In this panel, one can find that $\delta B_{p0} \sim 10^{-5}T$. And also, amplitude of the equilibrium magnetic field is $B_{\text{peq}} \sim 0.2T$. Then, QLMA and QLMB can be neglected in the derivation.

It should be noted that QLMC and nonlinear coupling terms are neglected in both theoretical analysis and simulation results. Furthermore, effects of plasma flow and viscosity are not included here. All these effects can may be dramatically influence the dynamics of FMR [36] and tearing mode [37] but are well beyond the scope of this work.

5. Summary and discussion

In this work, we have proposed a new analytical theory to unify the HKT linear and Rutherford quasi-linear solutions using the in-viscid two-field reduced MHD model. Via the quasi-linear approach [29], we obtained a closed system of equations for FMR response in the Taylor problem. It should be noted that the quasi-linear approach was proposed to reproduce the Rutherford equation and unify the linear exponential and quasi-linear algebraic growth of intrinsic tearing mode. One of the necessary assumptions used in [29], e.g. the expression of ϕ_1 , may be not appropriate for FMR response. To unify the HKT linear and Rutherford quasi-linear solutions, mathematical skills used in previous work should be extended. Transforming the quasi-linear term, i.e. QLJ in Eq. (7), into the exponential part of ϕ_1 and ψ_1 , the rearranged MHD equations can be solved as before [20]. Here, the terms of QLMA, QLMB, and QLMC in Eqs. (6)-(8) are neglected. Note that all those three terms are not needed to reproduce the Rutherford equation. From [29], the terms of QLMA and QLMB are important only in the regime where $W\Delta' \gg 1$. Such a regime is well beyond the scope of this work. In addition, our work can be straightforwardly extended to the cylindrical geometry.

Our FMR solution uniformly valid throughout the entire regimes from the HKT linear solution to the Rutherford quasi-linear solution. In particular, the quasi-linear effect can be described by a single coefficient K_s . When the quasi-linear index $K_s \propto S^{8/5}\psi_c^2 \rightarrow 0$, the HKT linear solution is recovered. On the other hand, the

quasi-linear effect cannot be neglected in the island growth when $K_s \sim 1$. We also numerically evaluated the expression of FMR. Results show that the normalized flux function ψ_{norm} decreases with K_s while the steady states of FMR satisfy that $\psi_{\text{norm}} = 1$. To verify the analytical solution of FMR, we developed a reduced MHD code. Results in our new analytical solution show good agreement with reduced MHD simulations. For example, when K_s is fixed in the reduced MHD code, we found that simulation results for different η are all agree with the theoretical expression of ψ_{norm} . Then, the quasi-linear effect in the reduced MHD simulation can also be described by the quasi-linear coefficient K_s . In addition, the effect of QLMA and QLMB on the FMR response can be neglected, which is consistent with our theoretical analysis.

Due to the limitation of the two-field reduced MHD model, many physics elements for the RMP-induced plasma response have not been included. For example, two-fluid and neo-classical effects are known to have strong influence over plasma response to RMPs near resonant surfaces[12, 13, 14, 38]. Furthermore, our derivation is appropriate only in the static plasma. We plan to address these important issues in future studies.

Acknowledgments

We thank Professor Ding Li for his helpful discussion. This work was supported by the Fundamental Research Funds for the Central Universities at Huazhong University of Science and Technology Grant No. 2019kfyXJJS193, the National Natural Science Foundation of China Grant Nos. 11775221 and No. 51821005, the Young Elite Scientists Sponsorship Program by CAST Grant No. 2017QNRC001, and U.S. Department of Energy Grant Nos. DE-FG02-86ER53218 and DE-SC0018001.

Appendix A. Derivation procedure of the Rutherford equation

To study the island evolution in the regime where $W \sim \delta_{\text{layer}}$, a pioneer theory was proposed by Rutherford [22]. In this appendix, we give a short review of the derivation of Rutherford equation. Using a Cartesian coordinate system (x, y, z) and introducing the flux function ψ and stream function ϕ , the magnetic field and the velocity can be written as $\vec{B} = \vec{e}_z \times \nabla\psi$ and $\vec{v} = \vec{e}_z \times \nabla\phi$. The incompressible two-field reduced MHD model governing ψ and F are given, respectively, by

$$\partial_t \psi + \vec{v} \cdot \nabla \psi = \eta J_z, \quad (\text{A.1})$$

$$\rho(\partial_t + \vec{v} \cdot \nabla) F = \vec{B} \cdot \nabla J_z. \quad (\text{A.2})$$

In the Rutherford regime, the inertial term in Eq. (A.2) can be neglected [22]. This assumption leads to $\vec{B} \cdot \nabla J_z = 0$, implying

$$J_z = J_z(\psi). \quad (\text{A.3})$$

As is shown in [29], see also in Appendix B, island evolution in such a regime cannot reduce to the linear exponential one since the inertial term is neglected. To unify the linear exponential and quasi-linear algebraic solution of tearing mode, one should contain the inertial term in Eq. (A.2). We also define $\psi = \psi(x, y, t) = \psi_{\text{eq}}(x) + \delta\psi(x, y, t) = \psi_{\text{eq}}(x) + \delta\psi_0 + \sum_{l=1}^{\infty} \psi_l \cos(lky)$ and $\phi = \phi(x, y, t) = \delta\phi(x, y, t) = \delta\phi_0 + \sum_{l=1}^{\infty} \phi_l \sin(lky)$ as usual. In the inner region, $B_{y\text{eq}} = \frac{d\psi_{\text{eq}}}{dx} \approx B'_y x$. Then, Eq. (A.2) reduces to

$$\partial_t \delta\psi - \frac{\partial \delta\phi}{\partial y} B'_y x = \eta(J_z - J_{\text{zeq}}). \quad (\text{A.4})$$

To eliminate $\delta\phi$, we divide x and average over y at constant ψ on Eq. (A.4) [22]. Then, the following equation can be obtained

$$J_z(\psi) - J_{\text{zeq}} = \eta^{-1} \left\langle \frac{\partial_t \delta\psi}{[\psi - \delta\psi]^{\frac{1}{2}}} \right\rangle / \langle [\psi - \delta\psi]^{-1/2} \rangle, \quad (\text{A.5})$$

where $\langle f \rangle = \frac{1}{2\pi} \int_0^{2\pi/k} f dy$.

Via the asymptotic matching, we obtain

$$\Delta'_l \psi_l = 2\mu_0 \left\langle \cos(lky) \int_{-\infty}^{\infty} \delta J_z dx \right\rangle, \quad (\text{A.6})$$

where $\Delta'_l = [\partial \ln \psi_l / \partial x]_{0-}^{0+}$. Combing Eqs. (A.5) and (A.6), the Rutherford equation can be obtained as following

$$\Delta' \psi_s = \frac{4A\mu_0}{\eta(2B'_y)^{\frac{1}{2}}} \psi_s^{\frac{1}{2}} \frac{\partial \psi_s}{\partial t}, \quad (\text{A.7})$$

where $\psi_s = \psi_1(x=0)$, $\Delta' = \Delta'_1$, and $A = A_R \approx 0.7$.

Appendix B. Unifying the linear exponential and Rutherford algebraic growth of tearing mode using Li's method

To connect the linear exponential and quasi-linear algebraic growth of tearing mode, Li proposed an unique quasi-linear approach [29]. In this appendix, we give a short review of Li's approach. Note that Li developed his approach in cylindrical geometry. To make a comparison with this work, we extend the original method to the two-dimensional slab geometry. We define $\psi = \psi_{\text{eq}} + \delta\psi$, $\phi = \delta\phi$, $\delta\psi = \sum_{l=0}^{\infty} \delta\psi_l = \delta\psi_0 + \sum_{l=1}^{\infty} \psi_l \cos(lky)$, and $\delta\phi = \sum_{l=0}^{\infty} \delta\phi_l = \delta\phi_0 + \sum_{l=1}^{\infty} \phi_l \sin(lky)$. Neglecting the higher harmonic coupling, Eqs. (1) and (2) can be reduced to the following forms

$$\partial_t \delta\psi_1 + \delta\vec{v}_1 \cdot \nabla \psi_{\text{eq}} + \underbrace{\delta\vec{v}_1 \cdot \nabla \delta\psi_0}_{\text{QLMA}} = \eta \delta J_{z1}, \quad (\text{B.1})$$

$$\underbrace{\rho \partial_t \delta F_1}_{\text{ITV}} = \vec{B}_{\text{eq}} \cdot \nabla \delta J_{z1} + \underbrace{\delta \vec{B}_1 \cdot \nabla J_{\text{zeq}}}_{\text{EQJD}} + \underbrace{\delta \vec{B}_0 \cdot \nabla \delta J_{z1}}_{\text{QLMB}} + \underbrace{\delta \vec{B}_1 \cdot \nabla \delta J_{z0}}_{\text{QLJ}}, \quad (\text{B.2})$$

$$\underbrace{\partial_t \delta\psi_0}_{\text{QLMC}} + \langle \delta\vec{v}_1 \cdot \nabla \delta\psi_1 \rangle = \eta \delta J_{z0}. \quad (\text{B.3})$$

Usually, effect of EQJD can be neglected in the inner region [33, 34].

To obtain the Rutherford equation, one should neglect terms of QLMA, QLMB, QLMC, and ITV in Eqs. (B.1)-(B.3) in the inner region [29]. Then, one arrives at

$$\partial_t \delta\psi_1 + \delta\vec{v}_1 \cdot \nabla \psi_{\text{eq}} = \eta \delta J_{z1}, \quad (\text{B.4})$$

$$0 = \vec{B}_{\text{eq}} \cdot \nabla \delta J_{z1} + \frac{1}{\eta} \delta \vec{B}_1 \cdot \nabla \langle \delta\vec{v}_1 \cdot \nabla \delta\psi_1 \rangle. \quad (\text{B.5})$$

Within the constant- ψ assumption, Eqs. (B.4) and (B.5) can be rearranged to

$$\partial_t \psi_s - k B'_y x \phi_1 = \eta J_{z1}, \quad (\text{B.6})$$

$$k B'_y x J_{z1} + \frac{k^2}{2\eta} \psi_s^2 \partial_x^2 \phi_1 = 0, \quad (\text{B.7})$$

where $\psi_s = \psi_1(x = 0)$. Combing Eqs. (B.6) and (B.7) and setting $\phi_1 = -\nu \partial_t \psi_s Y$, $Y = Y(\chi)$, and $x = \delta\chi$, one can obtain

$$\frac{d^2 Y}{d\chi^2} - \chi^2 Y = \chi, \quad (\text{B.8})$$

$$\delta^4 = \frac{\frac{1}{2} \psi_s^2}{(B'_y)^2}, \quad (\text{B.9})$$

$$\nu = \frac{1}{k B'_y \delta}. \quad (\text{B.10})$$

Solution of Eq. (B.8) is [29]

$$Y = -\frac{\chi}{2} \int_0^1 d\lambda (1 - \lambda^2)^{-\frac{1}{4}} \exp\left(-\frac{\lambda \chi^2}{2}\right). \quad (\text{B.11})$$

After asymptotic matching, the final expression of ψ_s is obtained

$$\Delta' \psi_s = \mu_0 \int J_{z1} dx$$

$$\begin{aligned}
 &= -\frac{\mu_0}{2\eta} \frac{k^2}{kB'_y} \psi_s^2 \int \frac{\partial_x^2 \phi_1}{x} dx \\
 &= \frac{C_0 \mu_0}{\eta} \delta \partial_t \psi_s \\
 &= \frac{4A\mu_0}{\eta} \frac{\psi_s^{\frac{1}{2}}}{\sqrt{2B'_y}} \partial_t \psi_s,
 \end{aligned} \tag{B.12}$$

$$\tag{B.13}$$

where

$$C_0 = \int_{-\infty}^{\infty} [1 + \chi Y] d\chi, \tag{B.14}$$

$$A = A_L = \frac{2^{\frac{1}{4}}}{4} C_0 \approx \frac{2^{\frac{1}{4}}}{4} \times 2.12 \approx 0.63. \tag{B.15}$$

Obviously, the Rutherford equation can be recovered via this quasi-linear approach except that $A = A_R \approx 0.7$ while $A = A_L \approx 0.63$ in Rutherford's and Li's approach, respectively. In addition, Li found a new algebraic growth of tearing mode when QLMA and QLMB are considered.

To connect the linear exponential and quasi-linear algebraic growth of tearing mode, ITV in Eq. (B.2) should be included. Then, one arrives at

$$\partial_t \delta \psi_1 + \delta \vec{v}_1 \cdot \nabla \psi_{\text{eq}} = \eta \delta J_{z1}, \tag{B.16}$$

$$\rho \partial_t \delta F_1 = \vec{B}_{\text{eq}} \cdot \nabla \delta J_{z1} + \underbrace{\frac{1}{\eta} \delta \vec{B}_1 \cdot \nabla \langle \delta \vec{v}_1 \cdot \nabla \delta \psi_1 \rangle}_{\text{QLJ}}. \tag{B.17}$$

To take a further step, we simplify Eqs. (B.16) and (B.17) to

$$\partial_t \psi_s - kB'_y x \phi_1 = \eta J_{z1}, \tag{B.18}$$

$$\rho \partial_t F_1 = -kB'_y x J_{z1} - \frac{k^2}{2\eta} \psi_s^2 \partial_x^2 \phi_1. \tag{B.19}$$

Setting $\phi_1 = -\frac{1}{kB'_y} \partial_t \psi_s \Phi$ and $\Phi = \Phi(x)$, one obtains

$$\frac{d^2 \Phi}{dx^2} \left[\partial_t + \frac{k^2}{2\rho\eta} \psi_s^2 \right] (\partial_t \psi_s) - \frac{(kB'_y)^2}{\rho\eta} x^2 \partial_t \psi_s \Phi = \frac{(kB'_y)^2}{\rho\eta} x \partial_t \psi_s. \tag{B.20}$$

Introducing $x = \delta_{\text{Li}} \chi$ and $\Phi = \delta_{\text{Li}}^{-1} Y(\chi)$, then Eq. (B.20) can be simplified to Eq. (B.8) and

$$\delta_{\text{Li}}^4 = \frac{\rho\eta}{(kB'_y)^2 \partial_t \psi_s} \left[\partial_t + \frac{k^2}{2\rho\eta} \psi_s^2 \right] (\partial_t \psi_s). \tag{B.21}$$

Via asymptotic matching, the following expression of ψ_s is obtained

$$\Delta' \psi_s = \mu_0 \int J_{z1} dx = \frac{C_0 \mu_0}{\eta} \delta_{\text{Li}} \partial_t \psi_s, \tag{B.22}$$

which leads to

$$(\Delta')^4 = \frac{\rho\eta}{(kB'_y)^2} \left[\partial_t \ln \psi_s + \frac{k^2}{2\rho\eta} \psi_s^2 \right] \left(\frac{C_0 \mu_0}{\eta} \partial_t \ln \psi_s \right)^4. \tag{B.23}$$

The linear and Rutherford regimes can be recovered when $\partial_t \ln \psi_s \gg \frac{k^2}{2\rho\eta} \psi_s^2$ and $\partial_t \ln \psi_s \ll \frac{k^2}{2\rho\eta} \psi_s^2$, respectively.

Appendix C. Comparison with a previous theory

In [29], Li unify the linear exponential and quasi-linear algebraic growth of tearing mode. Following their quasi-linear approach, we propose an integral form of FMR response which unify HKT linear and Rutherford quasi-linear solutions. Furthermore, one can find that Eq. (15) and Eq. (B.8) share the same form if we define $U = YG$. Then, it is necessary to clarify the difference between our work and previous one.

To solve the reduced MHD equations in the inner region, Li assumes that $\phi_1 = -\frac{1}{kB'_y} \partial_t \psi_s \Phi$ and $\Phi = \frac{Y}{\delta_{Li}}$, where $\chi = \frac{x}{\delta_{Li}}$, $\Phi = \Phi(\chi)$, and $Y = Y(\chi)$ [29]. Then,

$$\phi_1 = -\frac{1}{kB'_y} \partial_t \psi_s \delta_{Li}^{-1} Y(\chi) = -\frac{1}{kB'_y} \partial_t \psi_s \delta_{Li}^{-1} Y(\chi), \quad (C.1)$$

$$\delta_{Li}^4 = \frac{\rho\eta}{(kB'_y)^2 \partial_t \psi_s} [\partial_t + \frac{k^2}{2\rho\eta} \psi_s^2] (\partial_t \psi_s). \quad (C.2)$$

When $W \ll \delta_{Li}$, δ_{Li} satisfies that

$$\delta_{Li}^4 = \frac{\rho\eta}{(kB'_y)^2 \partial_t \psi_s} \partial_t^2 \psi_s = \frac{a^4 \tau_A^2}{(ka)^2 \tau_R} \frac{\partial_t^2 \psi_s}{\partial_t \psi_s} \approx \frac{a^4 \tau_A^2}{(ka)^2 \tau_R} \frac{\partial_t \psi_s}{\psi_s}. \quad (C.3)$$

For the FMR response, equations in the inner region should be solved using the Laplace transform [15]. From our derivation, ϕ_1 satisfies that

$$\phi_1 = -\frac{1}{kB_p} \mathcal{L}^{-1} \left[\frac{s\tilde{g}}{\delta_{RI}} Y(\chi) \right] = -\frac{1}{kB_p} \mathcal{L}^{-1} \left[\frac{s\tilde{\psi}_s - \mathcal{L}[(\frac{k^2}{2\rho\eta} \psi_s^2) \hat{\psi}_s]}{\delta_{RI}} Y(\chi) \right]. \quad (C.4)$$

In the linear limit, ϕ_1 can be expressed as

$$\phi_1 = -\frac{1}{kB_p} \mathcal{L}^{-1} \left[\frac{s\mathcal{L}(\psi_s)}{\delta_{RI}} Y(\chi) \right] = -\frac{1}{kaB'_y} \mathcal{L}^{-1} \left[\frac{s\mathcal{L}(\psi_s)}{\delta_{RI}} Y\left(\frac{x}{a\delta_{RI}}\right) \right], \quad (C.5)$$

where $B'_y = \frac{B_p}{a}$. If δ_{RI} does not dependent on s , i.e. the Laplace factor, one can rewrite Eq. (C.5) as

$$\phi_1 = -\frac{1}{kB'_y} \frac{Y(\chi)}{a\delta_{RI}} \mathcal{L}^{-1} [s\mathcal{L}(\psi_s)] = -\frac{1}{kB'_y} \frac{Y(\chi)}{a\delta_{RI}} \frac{\partial \psi_s}{\partial t}. \quad (C.6)$$

It is worth noting that $\delta_{RI}^4 = \frac{s\tau_A^2}{(ka)^2 \tau_R}$, i.e. $\delta_{RI} \propto s^{\frac{1}{4}}$, or, δ_{RI} is clearly dependent on s . Then, one cannot reduce Eq. (C.5) to Eq. (C.6). The final solutions of ϕ_1 are different from our work and previous one. Then, one of the necessary assumptions used in [29], i.e. expression of ϕ_1 , may be not appropriate for FMR even in the linear limit.

Based on above the discussion, one cannot expect that the unified theory uniformly connecting HKT linear and Rutherford quasi-linear solution can be obtained directly setting $\psi_s \Delta' = \psi_s \Delta'_0 + \psi_c \Delta'_e$ in Eq. (B.23).

References

- [1] Hu Q M, Yu Q, Rao B, Ding Y H, Hu X W, Zhuang G and the J-TEXT Team, 2011 Nucl. Fusion **52**, 083011
- [2] Hu Q M, Rao B, Yu Q, Ding Y H, Zhuang G, Jin W, and Hu X W, 2013 Phys. Plasmas **20**, 092502
- [3] Chen Z Y, Lin Z F, Huang D W, Tong R H, Hu Q M, Wei Y N, Yan W, Dai A J, Zhang X Q, Rao R, Yang Z J, Gao L, Dong Y B, Zeng L, Ding Y H, Wang Z J, Zhang M, Zhuang G, Liang Y, Pan Y, and Jiang Z H 2018 Nucl. Fusion **58** 082002
- [4] Ding Y H, Chen Z Y, Chen Z P, Yang Z J, Wang N C, Hu Q M, Rao B, Chen J, Cheng Z F, Gao L, Jiang Z H, Wang L, Wang Z J, Zhang X Q, Zheng W, Zhang M, Zhuang G, Yu Q Q, Liang Y F, Yu K X, Hu X W, Pan Y, and Gentle K W, 2018 Plasma Sci. Technol. **20** 125101
- [5] Evans T E, Moyer R A, Watkins J G, Osborne T H, Thomasand P R, Becoulet M, Boedo J A, Doyle E J, Fenstermacher M E, Finken K H, Groebner R J, Groth M, Harris J H, Jackson G L, La Haye R J, Lasnier C J, Masuzaki S, Ohyaabu N, Pretty D G, Reimerdes H, Rhodes T L, Rudakov D L, Schaffer M J, Wade M R, Wang G, West W P, and Zeng L 2005 Nucl. Fusion **45**, 595–607
- [6] Suttrop W, Eich T, Fuchs J C, Günter S, Janzer A, Herrmann A, Kallenbach A, Lang P T, Lunt T, Maraschek M, McDermott R M, Mlynec A, Pütterich T, Rott M, Vierle T, Wolfrum E, Yu Q, Zammuto I, and Zohm H. 2011 Phys. Rev. Lett. **106** 225004
- [7] Jakubowski M W, Evans T E, Fenstermacher M E, Groth M, Lasnier C J, Leonard A W, Schmitz O, Watkins J G, Eich T, Fundamenski W, Moyer R A, Wolf R C, Baylor L B, Boedo J A, Burrell K H, Frerichs H, deGrassie J S, Gohil P, Joseph I, Mordijck S, Lehnen M, Petty C C, Pinsker R I, Reiter D, Rhodes T L, Samm U, Schaffer M J, Snyder P B, Stoschus H, Osborne T, Unterberg B, Unterberg E, and West W P 2009 Nucl. Fusion **49**, 095013
- [8] Sun Y, Liang Y, Liu Y Q, Gu S, Yang X, Guo W, Shi T, Jia M, Wang L, Lyu B, Zhou C, Liu A, Zang Q, Liu H, Chu N, Wang H H, Zhang T, Qian J, Xu L, He K, Chen D, Shen B, Gong X, Ji X, Wang S, Qi M, Song Y, Yuan Q, Sheng Z, Gao G, Fu P, and Wan B 2016 Phys. Rev. Lett. **117**, 115001
- [9] Yang X, Sun Y W, Liu Y Q, Gu S, Liu Y, Wang H H, Zhou L N, and Guo W F 2016 Plasma Phys. Control. Fusion **58**, 114006
- [10] Yang X, Liu Y Q, Paz-Soldan C, Zhou L N, Li L, Xia G L, He Y L, and Wang S 2019 Nucl. Fusion **59**, 086012
- [11] Hu Q M, Nazikian R, Grierson B A, Logan N C, Park J K, Paz-Soldan C, and Yu Q 2019 Nucl. Fusion **26** 120702
- [12] Fitzpatrick R 2020 Phys. Plasmas **27** 042506
- [13] Fitzpatrick R and Nelson A O 2020 Phys. Plasmas **27** 072501
- [14] Fitzpatrick R 2020 Phys. Plasmas **27** 102511
- [15] Hahm T S and Kulsrud R M 1985 Phys. Fluids **28** 2412
- [16] Fitzpatrick R and Hender T C, 1991 Phys. Fluids B **3** 644
- [17] Fitzpatrick R 1998 Phys. Plasmas **5** 3325
- [18] Beidler M T, Callen J D, Hegna C C, and Sovinec C R 2017 Phys. Plasmas **24** 052508
- [19] Beidler M T, Callen J D, Hegna C C, and Sovinec C R 2018 Phys. Plasmas **25** 082507
- [20] Huang W L and Zhu P 2020 Phys. Plasmas **27** 022514
- [21] Huang W L, Zhu P, and Chen H 2020 Phys. Plasmas **27** 102514
- [22] Rutherford P H 1973 Phys. Fluids **16** 1903
- [23] Fitzpatrick R and Hender T C, 1991 Nucl. Fusion **33** 1049
- [24] Huang W L and Zhu P 2015 Phys. Plasmas **22** 032502
- [25] Huang W L and Zhu P 2016 Phys. Plasmas **23** 032505
- [26] Uenaga I, Furukawa M 2020 Phys. Plasmas **27** 092501
- [27] Luxon J 2002 Nucl. Fusion **42** 614
- [28] Fitzpatrick R 2014 Phys. Plasmas **21** 092513

- [29] Li D 1995 Phys. Plasmas **2** 3275
- [30] Xu J Q and Peng X D 2015 Phys. Plasmas **22** 102513
- [31] Wang X and Bhattacharjee A, 1992 Phys. Fluids B **4** 1795
- [32] Comisso L, Grasso D, and Waelbroeck F L 2015 Phys. Plasmas **22** 042109
- [33] Militello F, Huysmans G, Ottaviani M, and Porcelli F 2004 Phys. Plasmas **11** 125
- [34] Militello F, Borgogno D, Grasso D, Marchetto C, and Ottaviani M 2011 Phys. Plasmas **18** 112108
- [35] Furth H P, Killeen J, and Rosenbluth M N 1963 Phys. Fluids **6** 459
- [36] Li L, Liu Y Q, Loarte A, Schmitz O, Liang Y, and Zhong F C 2018 Phys. Plasmas **25** 082512
- [37] Ming Y and Zhou D 2017 Phys. Plasmas **24** 012509
- [38] Waelbroeck F L, Joseph I, Nardon E, Bécoulet M and Fitzpatrick R 2012 Nucl. Fusion **52** 074004

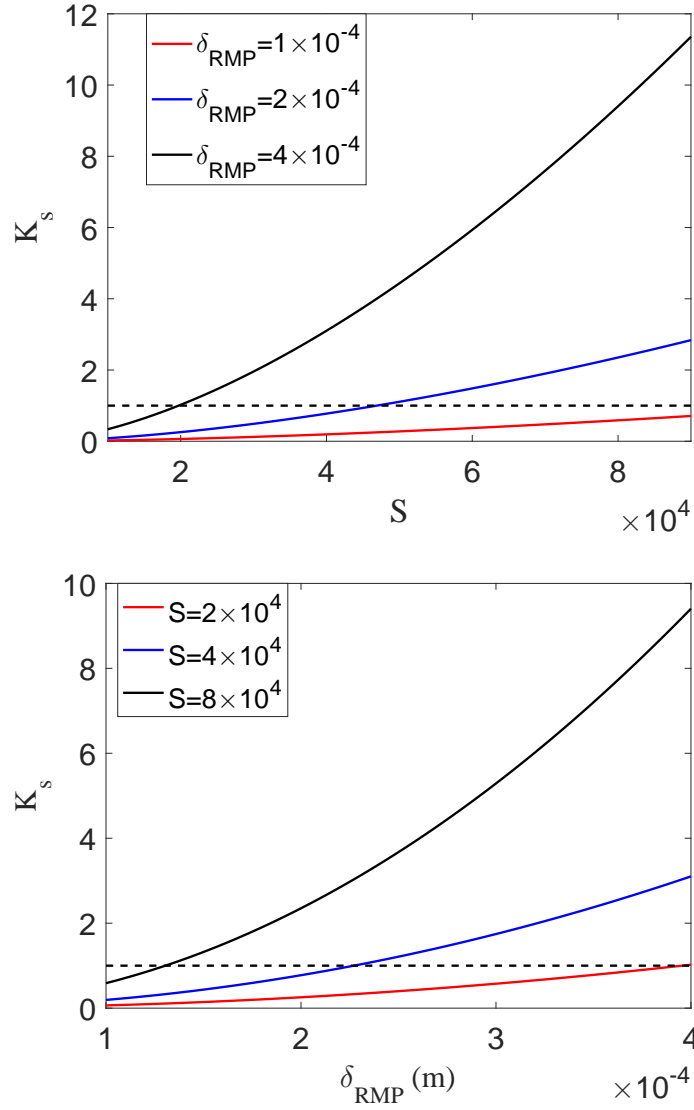


Figure 1: The upper and lower panels are dependence of K_s on Lunquist number for different δ_{RMP} and RMP amplitude for different S , respectively. The red, blue, and black curves in the upper (lower) panel represent $\delta_{\text{RMP}} = 1 \times 10^{-4} \text{m}$ ($S = 2 \times 10^4$), $\delta_{\text{RMP}} = 2 \times 10^{-4} \text{m}$ ($S = 4 \times 10^4$), and $\delta_{\text{RMP}} = 4 \times 10^{-4} \text{m}$ ($S = 8 \times 10^4$), respectively. The horizontal dashed lines in the upper and lower panels represent $K_s = 1$.

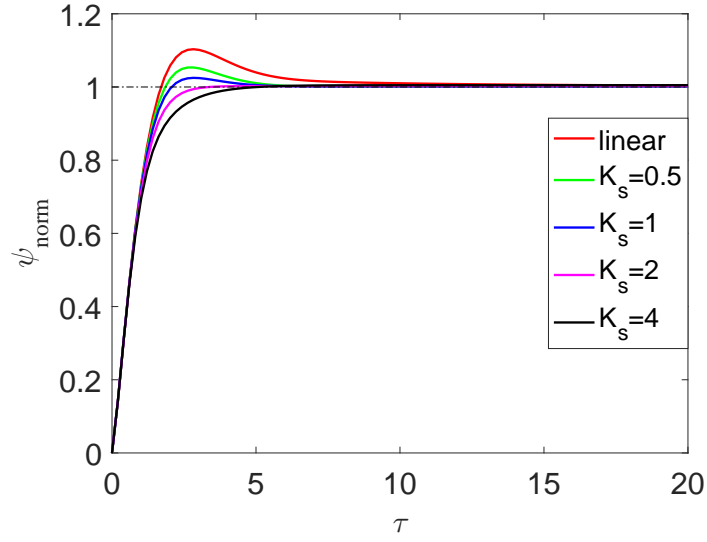


Figure 2: The normalized flux function as a function of τ ($\tau = \frac{t}{\tau_R^{\frac{3}{5}} \tau_A^{\frac{2}{5}}}$) for different K_s according to Eq. (19). The red, green, blue, magenta, and black curves represent $K_s = 0$, $K_s = 0.5$, $K_s = 1$, $K_s = 2$, and $K_s = 4$, respectively. The black horizontal line is $\psi_{\text{norm}} = 1$.

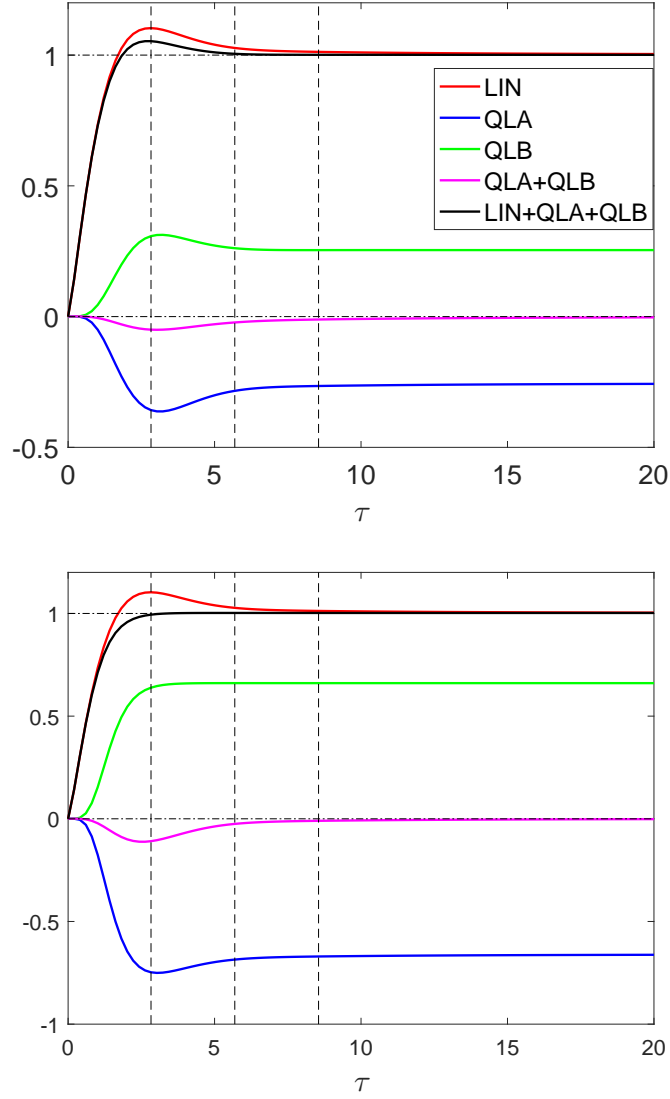


Figure 3: The upper and lower panels are different parts of Eq. (19) with $K_s = 0.5$ and $K_s = 2$. The red, blue, green, magenta, and black curves represent LIN, QLA, QLB, QLA + QLB, and LIN + QLA + QLB, respectively. The black vertical lines from left to right are $\tau = 2.83$, $\tau = 5.69$, and $\tau = 8.55$, respectively.

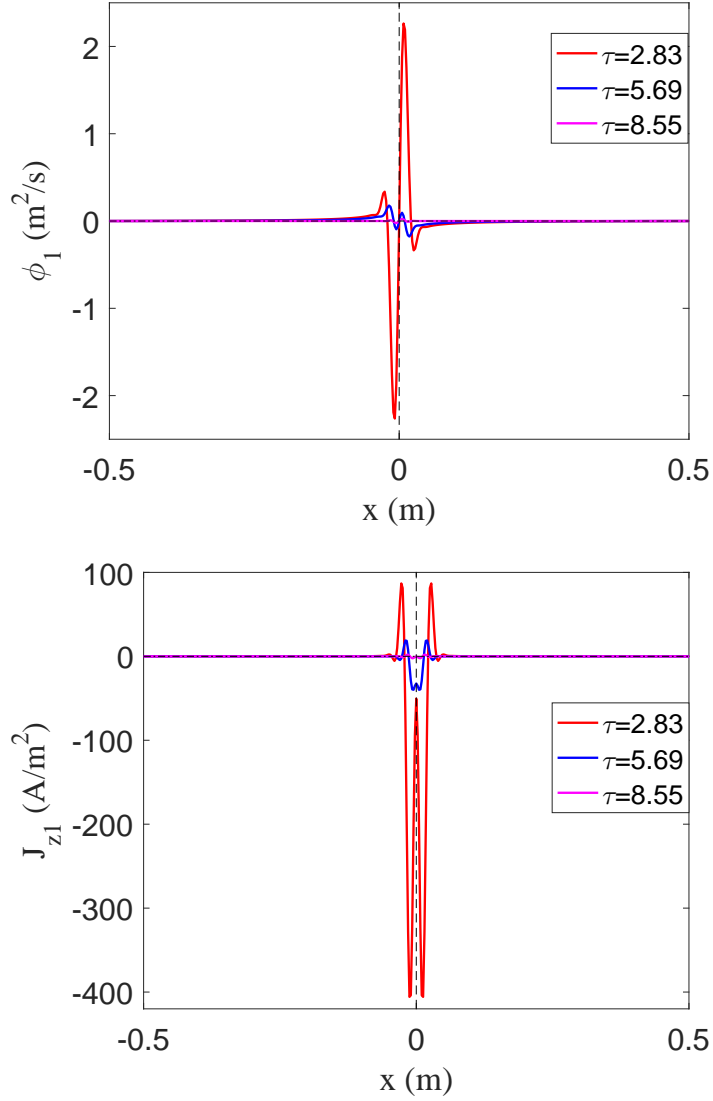


Figure 4: The upper and lower panels are distribution of ϕ_1 and J_{z1} at different time. The red, blue, and magenta curves represent $\tau = 2.83$, $\tau = 5.69$, and $\tau = 8.55$, respectively. The plasma resistivity and quasi-linear index used here are $\eta = 5 \times 10^{-5} \Omega m$ and $K_s = 0.5$.

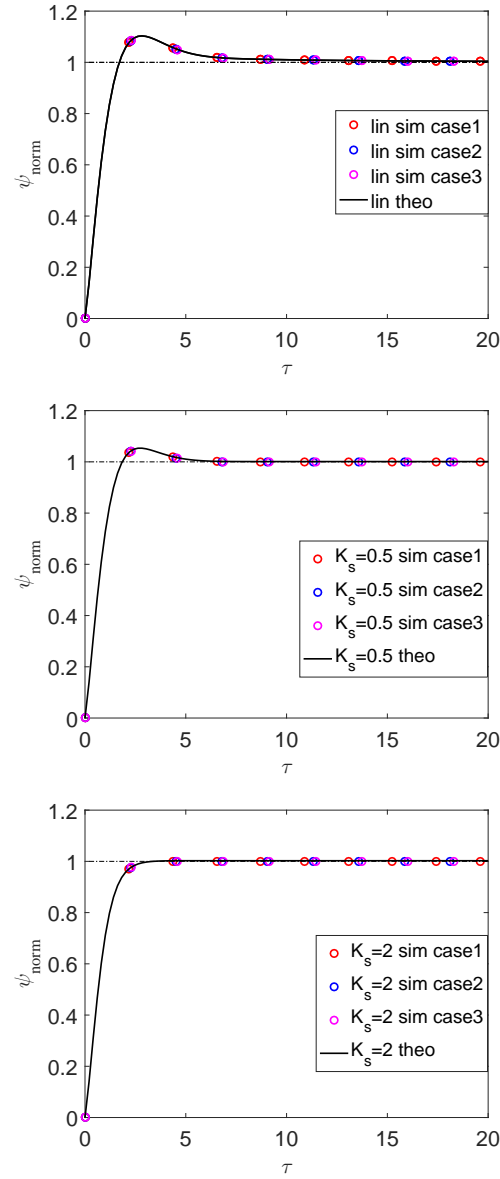


Figure 5: The top, middle, and bottom panels are dependence of ψ_{norm} on τ for $K_s = 0$, $K_s = 0.5$, and $K_s = 2$, respectively. The black curves are analytical results calculated from Eq. (19). The red, blue, and magenta cycles are simulation results with $\eta = 1 \times 10^{-5} \Omega m$ (case 1), $\eta = 2.5 \times 10^{-5} \Omega m$ (case 2), and $\eta = 5 \times 10^{-5} \Omega m$ (case 3), respectively.

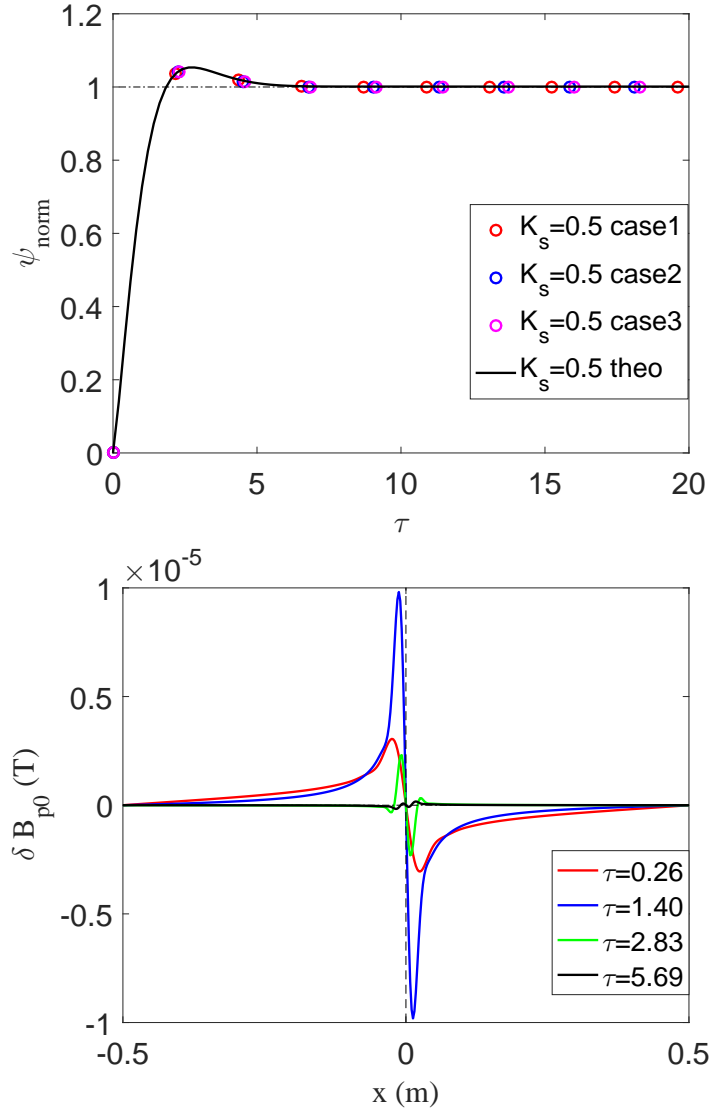


Figure 6: The upper and lower panels are dependence of ψ_{norm} on τ with different η and distribution of δB_{p0} at different time, respectively. The quasi-linear index used here is $K_s = 0.5$. The red, blue, and magenta cycles in the upper panel are simulation results of ψ_{norm} for $\eta = 1 \times 10^{-5} \Omega m$ (case 1), $\eta = 2.5 \times 10^{-5} \Omega m$ (case 2), and $\eta = 5 \times 10^{-5} \Omega m$ (case 3), respectively. The black curve is calculated from Eq. (19). In the lower panel ($\eta = 5 \times 10^{-5} \Omega m$), the red, blue, green, and black curves represent $\tau = 0.26$, $\tau = 1.40$, $\tau = 2.83$, and $\tau = 5.69$, respectively.